Efficient terahertz emission by mid-infrared laser pulses from gas targets

Wei-Min Wang,[1,2,*] Shigeo Kawata,[2] Zheng-Ming Sheng,[1,3] Yu-Tong Li,[1] Li-Ming Chen,[1] Lie-Jia Qian,[3] and Jie Zhang[1,3]

[1]*Beijing National Laboratory of Condensed Matter Physics, Institute of Physics, CAS, Beijing 100190, China*

[2]*Graduate School of Engineering, Utsunomiya University, 7-1-2 Yohtoh, Utsunomiya 321-8585, Japan*

[3]*Key Laboratory for Laser Plasmas of the Ministry of Education of China and Department of Physics, Shanghai Jiao Tong University, Shanghai 200240, China*

**Corresponding author: hbwwm1@iphy.ac.cn*

Received January 25, 2011; revised May 30, 2011; accepted June 10, 2011; posted June 13, 2011 (Doc. ID 141640); published July 11, 2011

It is shown by simulations that terahertz (THz) radiation can be produced more efficiently by a mid-infrared laser pulse from a gas target. The THz amplitude is enhanced by 35 times as the laser wavelength increases from 1 μm to 4 μm; a 4 μm laser at 10^{15} W cm^{-2} produces 5 MV/cm THz radiation. The THz amplitude changes oscillatingly with increasing laser intensity for a given laser wavelength. In addition, the laser intensity threshold for the THz emission is lower for a longer laser wavelength.

OCIS codes: 260.5210, 300.6495, 350.5610, 350.5400, 320.7120.

Terahertz (THz) waves with a field strength up to MV/cm or beyond are demanded by THz-pumped nonlinear physics and nonlinear THz spectroscopy, etc. Recent studies have shown that such THz radiation can be produced by intense laser pulses in gas and plasma targets [1–12]. For example, by employing the two-color laser scheme [3], it was demonstrated experimentally that THz radiation with the field strength of a few hundred kV/cm [5,8] was generated from gases. By applying a dc bias field to a gas plasma driven by a laser pulse, THz radiation was generated with the field strength determined by the bias amplitude available [11,12], which is generally at the level of tens of kV/cm.

So far most experimental and theoretical work on THz emission is based on using laser pulses of 0.8 μm wavelength. Nowadays, by either difference frequency generation or optical parametric amplification technologies, femtosecond intense mid-infrared lasers can be produced. Such laser pulses are used for high harmonic generation [13], which shows its prospects for brighter and more energetic attosecond bursts. Here, we consider THz generation by the use of mid-infrared laser pulses. We show numerically the possibility of producing tens of MV/cm THz radiation with such lasers in tenuous gas targets. The THz radiation generated in this way can be much stronger than that from the two-color laser scheme [5,10] at the same laser intensity, although the THz emission in both schemes results from asymmetric gas ionization. For the latter, the second harmonic light breaks the symmetry of the fundamental light ionization of gas [8,10]. In the mid-infrared laser scheme, by increasing the laser wavelength, the number of laser cycles ionizing the gas is reduced. Therefore, the higher asymmetry of the ionization makes it possible to trigger stronger net ionizing currents and more powerful THz radiation.

Let us consider that a laser pulse illuminates upon a tenuous gas. The laser with linear polarization along the z direction propagates along the $+x$ direction. Its vector potential A_z is the function of $\xi = ct - x$, where c is the speed of light in a vacuum. When the laser passes through the gas, it produces free electrons from gas atoms by field ionization. Assume that the velocities of the free electrons are zero at the moment they are produced from ionization. Therefore, a free electron marked by j gains the velocity $v_{zj} = -eA_z(\xi_j)/m_e c$ after the passage of the laser [10], where ξ_j is determined by the electron position and time when it was born; e is the electron charge; and m_e is the electron rest mass. Then the average velocity of these electrons is

$$\langle v_{z0} \rangle = \frac{-e}{m_e c N} \sum_{j=1}^{N} A_z(\xi_j), \tag{1}$$

where N is the total number of free electrons. Then a net current is formed and converted into THz radiation at the plasma oscillation frequency [10,12] where the THz amplitude scales linearly with $\langle v_{z0} \rangle$ [10]. When the laser is weak, the ionization occurs around the laser intensity peak and the newly born electron number is small and proportional to the local laser intensity. Therefore, the number distribution of newly born electrons versus the electron birth position ξ is symmetric with the center at the laser intensity peak. Then $\langle v_{z0} \rangle$ is zero, and thus no THz radiation can be generated, as usually encountered. While the laser is intense enough that the laser leading edge can ionize the gas completely, the symmetry of the number distribution of newly born electrons versus the electron birth position ξ breaks. As a result, $\langle v_{z0} \rangle$ deviates from zero, and THz radiation is generated. Therefore, even a single laser pulse can produce THz radiation when it is intense enough.

With the increase in the laser wavelength, the laser cycle number needed to ionize the gas completely is decreased, the electron number distribution versus the electron birth position tends to be more highly asymmetric, and $\langle v_{z0} \rangle$ becomes larger. In particular, for the laser of a long enough wavelength, the gas can be ionized completely by half-cycle; all $A_z(\xi_j)$ have the same sign; and then $\langle v_{z0} \rangle$ becomes very large. This leads to the generation of strong net current and subsequent powerful THz radiation.

We present two-dimensional (2D) particle-in-cell (PIC) simulations. Our PIC code includes 2D coordinates (x, y) and full momentum spaces (p_x, p_y, p_z). The field ionization is calculated by the ADK formula [14]. We take a hydrogen target with a trapezoidal density profile: $5\,\mu$m linear increase, $90\,\mu$m plateau, and $5\,\mu$m linear decrease. The gas density of the plateau region is $0.6 \times 10^{18}\,\mathrm{cm}^{-3}$, which can be completely ionized to be plasma with the electron density $n_e = 1.2 \times 10^{18}\,\mathrm{cm}^{-3}$ (or $\omega_p/2\pi = 10\,$THz, where $\omega_p = \sqrt{4\pi e^2 n_e/m_e}$ is the plasma oscillation frequency). To save the computational expense, we adopt a plane laser. This simplification is suitable for an intense laser with relatively large spot sizes when the gas can be fully ionized in the focused area. Otherwise, one needs to consider the effect of different plasma and radiation frequencies across the laser pulse. The laser polarized along the z direction propagates in the $+x$ direction. Its electric field takes the form of $E_z = E_0 \exp(-\xi^2/\tau_0^2) \sin(k\xi + \theta)$ with $\tau_0 = 9\,\mu$m or the FWHM duration of 50 fs, where θ is the carrier–envelope (CE) phase, $k = 2\pi/\lambda$, and λ is the wavelength.

Figures 1(a)–1(c) plot the amplitude of the produced THz radiation versus the intensity of the laser with different wavelengths. One can see that the maximal amplitude of the THz radiation generated by $4\,\mu$m lasers is much larger than that produced by $1\,\mu$m and $2\,\mu$m lasers. The maximal THz amplitudes are 0.32, 3.2, and 11.4 MV/cm for the lasers with wavelengths of 1, 2, and $4\,\mu$m, respectively. Therefore, a laser of a longer wavelength is capable of producing stronger THz radiation. In particular, the $4\,\mu$m laser at $1.2 \times 10^{15}\,\mathrm{W\,cm}^{-2}$ generates 5.3 MV/cm THz radiation.

It is also observed in Figs. 1(a)–1(c) that the THz amplitude does not enhance monotonically with the increasing laser intensity. Instead, it changes oscillatingly. The oscillation period is longer for the laser with a longer wavelength. In addition, the oscillation period becomes longer as the laser intensity enhances. One notices that the x axis adopts an exponential scale.

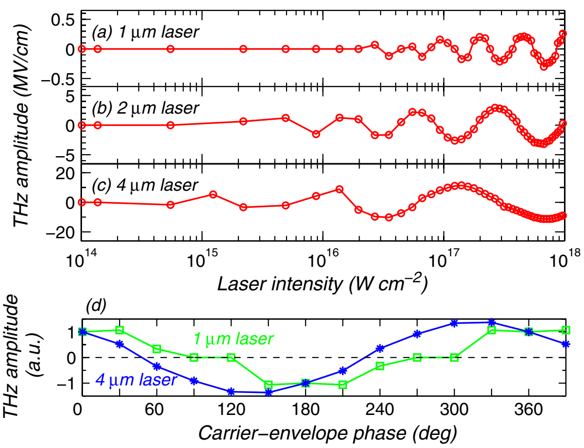

Fig. 1. (Color online) (a), (b), and (c): THz amplitude versus the intensity of the laser with different wavelengths, where the laser CE phase is zero. (d) THz amplitude versus the CE phase of the laser with different wavelengths, where the laser intensity is $10^{17}\,\mathrm{W\,cm}^{-2}$.

We explain the results above through Fig. 2, which displays the number distribution of newly born electrons versus the electron birth position. When $I_0 \geq 3.5 \times 10^{16}\,\mathrm{W\,cm}^{-2}$, only one cycle of the $4\,\mu$m lasers ionizes the gas completely (our simulations show that a half-cycle of the $8\,\mu$m lasers can ionize the gas completely; however, the reflected light is strong to the level of the produced THz radiation and therefore we do not present the results here), which is less than the cycle number of the $1\,\mu$m lasers ionizing the gas completely. Thus the $4\,\mu$m lasers tend to produce stronger THz radiation. From Fig. 1(c) it is observed that the negative peak, zero, and the positive peak of the THz amplitude appear at 3.5, 5.5, and $12 \times 10^{16}\,\mathrm{W\,cm}^{-2}$, respectively. From the corresponding plots in Fig. 2(a), one can see that when the positive and negative peaks of the THz amplitude rise, the number of free electrons produced from the laser half-cycle with the higher laser intensity is much larger than the one from the half-cycle with the lower intensity; otherwise, the THz amplitude is near zero. From the negative peak to the positive peak of the THz amplitude (or as the oscillation of the THz amplitude with increasing laser intensity experiences half a period), the laser envelope $ct - x$ ionizing the gas shifts backward by half a laser cycle. This explains the observation in Fig. 1 that the oscillation period of the THz amplitude with the laser intensity is longer for a laser of longer wavelength. This also explains that the oscillation period grows with the increasing laser intensity, since the decrease of the laser intensity $\exp(-2\xi^2/\tau_0^2)$ with the increase of $|\xi|$ grows gradually when $|\xi| > \tau_0/2$.

Hence, one can understand the results shown in Fig. 1(d) that the THz amplitude E_{THz} follows $E_{\mathrm{THz}}(\theta) = -E_{\mathrm{THz}}(\theta + \pi)$, since as the CE phase θ varies by π, the number distribution of newly born electrons versus their

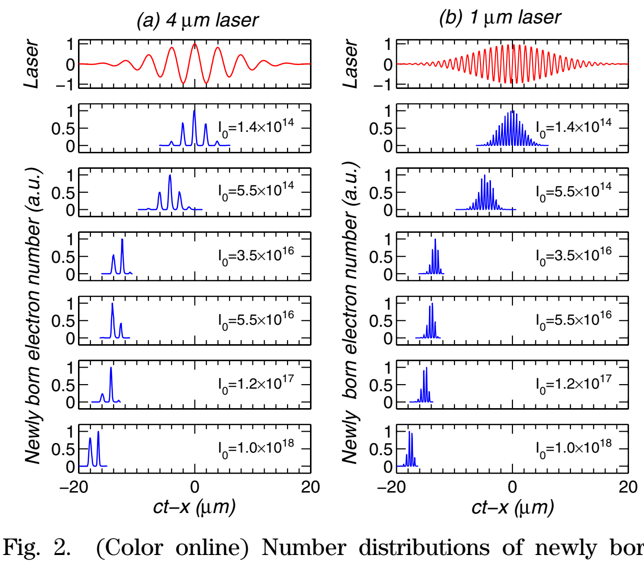

Fig. 2. (Color online) Number distributions of newly born electrons versus $ct - x$ for different laser intensities I_0, where t and x are the time and positions when electrons are born. Left column (a) results for $4\,\mu$m lasers; right column (b) for $1\,\mu$m lasers. The first row in each columns is the waveform of the laser electric field normalized by its amplitude. The laser CE phases are zero for both cases.

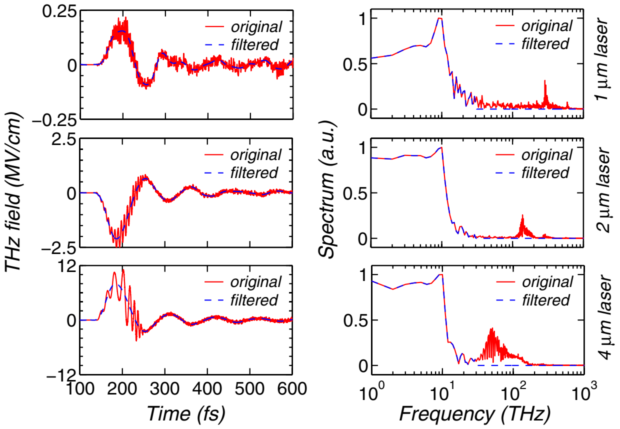

Fig. 3. (Color online) Left column, waveforms of the THz electric fields for different laser wavelengths; right column, corresponding spectra. The solid curves in every plot are the results from the original data of the simulations. The broken curves are the results after the components higher than 30 THz are filtered.

birth position remains unchanged, but the electron average velocity $\langle v_{z0} \rangle$ changes its sign. From this one can easily obtain $E_{\mathrm{THz}}(\theta) = E_{\mathrm{THz}}(\theta + 2\pi)$, which is also found in Fig. 1(d). This figure also shows that the THz radiation is affected by the CE phase even in the case of a large laser duration.

From Figs. 2(a) and 2(b), one can see that when the laser intensity is 1.4×10^{14} W cm^{-2}, the number distributions are symmetric with the centers at the laser pulse peaks and therefore no THz radiation is produced, as shown in Figs. 1(a) and 1(c). When the laser intensity is enhanced to 5.5×10^{14} W cm^{-2}, the peaks of the number distributions deviate from the laser pulse peaks. The 4 μm laser produces THz radiation [see Fig. 1(c)]. However, no THz radiation is produced by the 1 μm laser [see Fig. 1(a)]. This is because the ionization arises in many cycles of the 1 μm laser and the net currents formed by the positive half-cycles and the negative half-cycles tend to counteract each other. As a result, the laser intensity threshold for THz radiation generation is lower for a laser of a longer wavelength, as shown in Figs. 1(a)–1(c).

To obtain the THz amplitude values shown in Fig. 1, we have filtered the produced radiation components higher than 30 THz. We take the results with 10^{17} W cm^{-2} lasers with the CE phase of zero as an example, which are shown in Fig. 3. One can see that the waveforms are kept well after they are filtered. The THz waves have a main frequency around $\omega_p = 10$ THz. Among the spectrum components higher than 10 THz, the peaks appear at about the laser frequencies, which are the waves reflected by the plasma just formed. The reflected waves for the longer laser wavelength are stronger, which is consistent with the fact that a laser of a lower frequency is reflected more strongly by a plasma with the same density.

In conclusion, we have demonstrated that generally stronger THz radiation can be produced by lasers of longer wavelengths, even though for a given laser wavelength the THz radiation amplitude does not show monotonic increase with the laser intensity. The laser intensity threshold for THz radiation generation appears lower with longer laser wavelengths. With these advantages, a mid-infrared laser pulse is favorable for the generation of strong THz sources.

This work is supported in part by the National Science Foundation of China (NSFC), grants 10734130 and 10925421; the National Basic Research Program of China, grants 2007CB310406, 2007CB815100, and 2009GB105002; the Japan Society for the Promotion of Science (JSPS) and the Ministry of Education, Culture, Sports, Science and Technology (MEXT) in Japan; and the Center for Optical Research and Education (CORE) program at Utsunomiya University, Japan.

References

1. Z.-M. Sheng, K. Mima, J. Zhang, and H. Sanuki, Phys. Rev. Lett. **94**, 095003 (2005).
2. Z.-M. Sheng, H.-C. Wu, K. Li, and J. Zhang, Phys. Rev. E **69**, 025401(R) (2004).
3. D. J. Cook and R. M. Hochstrasser, Opt. Lett. **25**, 1210 (2000).
4. M. Kress, T. Loffler, S. Eden, M. Thomson, and H. G. Roskos, Opt. Lett. **29**, 1120 (2004).
5. T. Bartel, P. Gaal, K. Reimann, M. Woerner, and T. Elsaesser, Opt. Lett. **30**, 2805 (2005).
6. X. Xie, J. Dai, and X.-C. Zhang, Phys. Rev. Lett. **96**, 075005 (2006).
7. J. Dai, N. Karpowicz, and X.-C. Zhang, Phys. Rev. Lett. **103**, 023001 (2009).
8. K. Y. Kim, J. H. Glownia, A. J. Taylor, and G. Rodriguez, Opt. Express **15**, 4577 (2007).
9. H.-C. Wu, J. Meyer-ter-Vehn, and Z.-M. Sheng, New J. Phys. **10**, 043001 (2008).
10. W.-M. Wang, Z.-M. Sheng, H.-C. Wu, M. Chen, C. Li, J. Zhang, and K. Mima, Opt. Express **16**, 16999 (2008).
11. A. Houard, Y. Liu, B. Prade, V. T. Tikhonchuk, and A. Mysyrowicz, Phys. Rev. Lett. **100**, 255006 (2008).
12. W.-M. Wang, Z.-M. Sheng, X.-G. Dong, H.-W. Du, Y.-T. Li, and J. Zhang, J. Appl. Phys. **107**, 023113 (2010).
13. P. Agostini and L. F. DiMauro, Contemp. Phys. **49**, 179 (2008).
14. M. V. Ammosov, N. B. Delone, and V. P. Krainov, Sov. Phys. JETP **64**, 1191 (1986).